A Nanocrystal-based Ratiometric pH Sensor for Natural pH Ranges

Rebecca C. Somers[a], **Ryan M. Lanning**[b], **Preston T. Snee**[c], **Andrew B. Greytak**[d], **Rakesh K. Jain**[b], **Moungi G. Bawendi**[a], and **Daniel G. Nocera**[a]

Rakesh K. Jain: jain@steele.mgh.harvard.edu; Moungi G. Bawendi: mgb@mit.edu; Daniel G. Nocera: nocera@mit.edu

[a]Department of Chemistry, Massachusetts Institute of Technology, 77 Massachusetts Avenue, Cambridge, MA, 02139-4307, USA

[b]Edwin L. Steele Laboratory for Tumor Biology, Department of Radiation Oncology, Massachusetts General Hospital and Harvard Medical School, 100 Blossom Street, Cox-7, Boston, MA 02114, USA

Summary

A ratiometric fluorescent pH sensor based on CdSe/CdZnS nanocrystal quantum dots (NCs) has been designed for biological pH ranges. The construct is formed from the conjugation of a pH dye (SNARF) to NCs coated with a poly(amido amine) (PAMAM) dendrimer. The sensor exhibits a well–resolved ratio response at pH values between 6 and 8 under linear or two–photon excitation, and in the presence of a 4% bovine serum albumin (BSA) solution.

Introduction

Inorganic semiconductor nanocrystals (NCs), also known as quantum dots, have been widely pursued as components of optical sensors due to their attractive properties of narrow, tunable emission, continuous excitation spectra, high molar extinction coefficients and photoluminescence (PL) quantum yields, and resistance to photobleaching.[1–9] The favorable photophysical properties of NCs compared to organic fluorophores make them suitable candidates for incorporation into a sensing strategy that modulates the luminescence of NCs. Fluorescence Resonant Energy Transfer (FRET) is often used as the means to control luminescence, and NCs have been investigated as both FRET donors and acceptors;[1,10–12] however, most examples of FRET–based NC sensor mechanisms take advantage of the NC as the donor, which has led to the demonstration of NC sensors for a variety of target analytes.[2,4,13,14]

Emission–ratiometric behavior is a desirable for optical sensors because it allows the ratio signal to be read independently of probe concentration or excitation intensity.[15] We

Correspondence to: Moungi G. Bawendi, mgb@mit.edu; Daniel G. Nocera, nocera@mit.edu.

[c]Current Address: Department of Chemistry, University of Illinois at Chicago, 845 West Taylor Street, MC 111, Chicago IL, 60607

[d]Current Address: Department of Chemistry and Biochemistry, University of South Carolina, Columbia, SC 29208

[†]Electronic Supplementary Information (ESI) available: Full experimental details and characterization of NC-SNARF construct, spectroscopic methods, and emission spectra and lifetime traces of NC-SNARF construct.

previously reported[3,4] the first example of a CdSe/ZnS NC–based ratiometric and reversible pH sensor, which was synthesized through the conjugation of an emissive squaraine pH–sensitive dye to the NC.[4] By engineering the construct so that the emission of the NC overlaps with the pH–dependent absorption of the squaraine dye, FRET from the NC donor to the dye acceptor was modulated by pH, resulting in a change in the ratio of wavelength–resolved PL emission from the NC and dye, with an isosbestic point in between. While this work represented a proof–of–concept for a general method towards ratiometric NC sensors for various targets,[1,16] the pH range ($pK_a \sim 8.8$) of sensor response was incompatible with biological applications.[17,18] Moreover the biological utility of the NC construct was limited owing to the potential lability of the ester bond linking the dye to the NC towards esterases.[19] We therefore sought to design a NC–chemosensor construct that would be robust toward degradation and exhibit signal transduction in a pH range of pertinence to biology. Here we describe the use of poly(amido amine) (PAMAM) dendrimer ligands and an acceptor dye (SNARF–5F) to afford the following properties: (i) a chemosensing response in the pH 7 range; (ii) a "starburst" structure that furnishes a high degree of valency for coupling of multiple dye substituents per NC; (iii) amine pendants to furnish robust amide bonds upon conjugation; and, (iv) the exploitation of the high two–photon absorption cross–section of NC[20] to establish the chemosensing response. With regard to the latter, two-photon excitation allows for minimal scattering of excitation light and hence significant depth penetration,[21,22] diminished photodamage and excitation of probes confined to a small volumes.[22–24] These properties are especially valuable for biological imaging and sensing[25] especially in tumor microenvironments,[26] which is of particular interest to us.[17] Together, the results reported herein, furnish a NC-chemosensing construct that operates in the biological pK_a range under two-photon excitation conditions.

Experimental

CdSe NCs overcoated with alloyed CdZnS were prepared by a modified literature method.[27,28] Reagent doses for the overcoat were chosen to yield a ~3 monolayer shell on the bare CdSe NCs as previously described.[28] The quantum yield of the NC sample was Φ= 58% in hexanes after one precipitation, with a FWHM = 32 nm. The lowest energy absorption peak was at 508 nm.

Dihydrolipoic acid–modified poly(amido amine) (DHLA–PAMAM) was prepared by coupling generation 1 PAMAM to DHLA, which was prepared by literature methods,[29] in the presence of EDC and NHS. Cap–exchange of CdSe/CdZnS with DHLA–PAMAM was accomplished by mixing DHLA–PAMAM in methanol with chloroform solution of NCs. The dendrimer solubilized NCs were extracted into water and excess ligands were removed through dialysis using Millipore centrifuge tubes equipped with 50,000 Da molecular weight cut–off (MWCO) filters. The isolated aqueous compatible NCs were found to have a quantum yield of $\Phi = 26\%$ in water and a FWHM = 32 nm. SNARF–5F 5 (and –6) were conjugated to the DHLA–PAMAM modified NCs by activating the carboxylic acid of the dye for amide coupling with 1–ethyl–3,3′–dimethylaminopropylcarbodiimide (EDC) in pH 6 MES buffer. The N–hydroxysuccinimide (NHS) activated dye was coupled to DHLA-PAMAM solubilized NC with stirring. The unreacted dye was removed through dialysis with 50,000 Da MWCO filters.

Samples for UV–vis spectra were prepared by diluting in appropriate standard pH phosphate buffers for pH 6–8 and a borate buffer for pH 9. Potassium phosphate buffered solution with 4%–bovine serum albumin (BSA) was used for calibration studies. Samples for light scattering measurements were filtered through a 0.2 μm syringe filter and microcentrifuged before measurements were taken at 25 °C. Steady–state fluorescence measurements were obtained in a 1 cm path length cuvette from a custom–built Photon Technology Instruments fluorometer installed with a Hamamatsu R928 photomultiplier tube and a 150 W Xe excitation lamp. Quantum yield (Φ) measurements were made by using rhodamine 590 as the reference. A 400 nm emitting Ti: Sapphire laser equipped with a gated intensified CCD camera was used to obtain time–resolved fluorescence spectra. Data were collected at room temperature using a 1 cm optical path fluorescence cuvette.

Two photon emission spectra were taken on NC–SNARF solutions prepared in potassium phosphate buffers with 4% BSA. Buffered sample solutions were placed in 0.1×1 mm^{22} inner diameter glass microslides attached to a standard microscope slide. All spectral measurements were taken on a custom–built multiphoton laser scanning microscope (MPLSM) with the emission output fibre–coupled to a spectrometer. Multiphoton excitation was performed by a Spectra–Physics Broadband MaiTai diode pumped Ti:Sapphire laser using 800–920 nm light at sample powers ranging from 10–60 mW. Two–photon laser scanning microscopy imaging was performed on an Olympus Fluoview 300 Laser Scanning Microscope modified with a Spectra–Physics MaiTai laser. All images were taken at either 800 or 850 nm with excitation powers of 42 or 35 mW, respectively.

The efficiency (E) of energy transfer was determined using the Förster equation,

$$\mathrm{E} = \frac{mk_{D \to A}}{mk_{D \to A} + \tau_D^{-1}} = \frac{mR_0^6}{mR_0^6 + r^6} \quad (1)$$

where τ_D is the donor excited–state decay lifetime, and $k_{D \to A}$ is there energy transfer rate. R_0 is the characteristic distance at which $k_{D \to A} = \tau_D^{-1}$ such that $E = 50\%$. Parametrs for the fit are given in the ESI. For a given sample, E can be obtained from the quenching of the NC donor emission intensity with respect to a control prepared with no dye. The efficiency was also obtained using the emission lifetimes of the donor in the absence (τ_D) and the presence of an acceptor (τ_{DA})

$$\mathrm{E} = 1 - \frac{\tau_{DA}}{\tau_D} \quad (2)$$

Details of synthesis, measurements and analysis are provided in ESI.

Results

We sought to prepare water–soluble NCs with a strongly bound PAMAM dendrimer coating. Dendrimer–capped NCs derived from PAMAM are known with monodentate thiol ligand coordination.[30,31] However, the monodentate coordination limits stability, which can be improved significantly by using multidentate thiol coordination.[32–34] To this end, we

modified PAMAM dendrimers bidentate dihydrolipoic acid as a NC surface chelating ligand as shown in Scheme 1. Ligand exchange of the NCs was accomplished by a facile phase–exchange method, as shown in Scheme 2, where distilled water was layered on top of a vigorously stirred chloroform/methanol solution of NCs and dendrimer ligand. Over the course of few hours, the colorful NC phase transfers to the top aqueous layer, leaving excess ligands in the organic phase. After water solubilization, NCs exhibiting appreciable quantum yield (26%) were obtained. NCs capped with DHLA–PAMAM ligands were also found to be stable for months when stored at 4 °C.

The EDC–mediated coupling of the SNARF–5F to the surface of the NCs was performed in distilled water. The use of the bicarbonate buffer system, conventional in peptide coupling chemistry, resulted in poor coupling yields and precipitation of the amine–terminated NCs. Conversely, a high coupling efficiency was achieved in distilled water owing to the high valency of the amines on the NCs. The yield of the reaction was as high as 86%, after removing unbound dye by repeated dialysis with water via ultracentrifugation. The hydrodynamic radius of the dendrimer capped NCs was determined through light scattering measurements and was observed to be 16 ± 1 nm. The hydrodynamic radius is larger than expected for a NC coated by a single layer of DHLA-PAMAM ligand but could be explained by a limited amount of cross-linking via disulfide bonds to give multiple PAMAM layers of the NC. The pK_a of a primary amine on a generation 1 PAMAM dendrimer is 9.00.[35] Thus in biological environments the PAMAM amine is likley protonated. We have found that the NCs are stable at pHs as high as 9; at and above pH 9, the NCs slowly precipitate over the course of one week.

The UV–vis absorption spectrum at each pH value (Fig 1) is the composite sum of the continuous NC absorption in the higher energies and of the pH dependent SNARF–5F absorption between 470–620 nm. By separating the NC and the dye contributions to the overall conjugate spectrum, a ratio of dye to NC of 26 to 1 was obtained. In the FRET analysis that follows, we take this to be the number of acceptors m per donor, assuming that all uncoupled dye has been removed in the dialysis steps.

The critical transfer distances at pH 6 and 9 were calculated using the quantum yield of NCs in absence of appended dye ($\varphi_D = 0.26$, measured by comparison to laser dye standards). Depending on the degree of spectral overlap, which is modulated by the pH, the critical transfer distance (R_0) was found to be between 4.46 nm (at pH 6) and 4.68 nm (at pH 9), typical for Förster energy transfer processes. Using Eq. 1, we can determine the NC-dye separation with a characteristic distance with the caveat that the conjugate chemistry gives a range of donor-acceptor separation distances and thus the characteristic distance that we obtain is necessarily a weighted average of these values.

Steady–state emission (Fig 2) exhibits spectra that are indicative of FRET that is pH dependent. While the construct was excited at $\lambda_{exc} = 365$ nm, where the SNARF–5F has little absorption, dye emission is clearly evident. In addition, the SNARF–5F becomes more absorptive at the NC emission wavelength as the pH is increased, thus increasing the spectral overlap between the donor–acceptor pair. As such, the donor NC emission is decreased, which is also a signature of energy transfer. The emission profiles of the

construct shown in Fig 2 are clearly ratiometric and unique over a range of pH. As shown in Fig 3, the sensor's quantum yield is such that the photoluminescence response to pH is clearly visible to the eye.

The emission of a two–color ratiometric sensor has ratio and intensity as two independent variables.[15,16] The state of the sensor can thus be determined from the ratio of any two wavelength–resolved emission channels that display significantly different intensity responses to pH. A calibration curve can be constructed using the ratio of the maximum emission intensities of the NC and dye or by using the ratio of the integrated intensity within two wavelength regions selected to capture each peak. Fig S1a illustrates an example calibration of the SNARF:NC ratio vs pH constructed from integrated emission spectra. The ratio monotonically increases from pH 6.0 to pH 8.0.

FRET was confirmed by time–resolved emission spectroscopy. Lifetimes decays are shown in Fig S2; the time constants as well as FRET parameters extracted from the lifetimes, are listed in Table 1. The lifetimes of the unconjugated NC was found to be 16 ns at pH = 6. The lifetime of the donor NC conjugated to SNARF is shortened owing to energy transfer. Moreover, the lifetime decay is pH dependent owing to enhanced energy transfer with increasing pH due to greater spectral overlap.

With lifetime quenching rate constants in hand, the energy transfer efficiency can be extracted from the emission lifetimes of the donor in the absence and the presence of an acceptor, er eq. (2). FRET is most efficient (37.5%) under basic conditions and decreases to 25% at pH 6, consistent with decreased spectral overlap between the donor–acceptor as the pH is lowered. A value for the donor–acceptor distance, r, can be calculated from from eq. (1). At a dye to NC ratio of 26:1, the distance between the SNARF and NC was 8.7 nm at pH 9 as compared to 9.6 nm at pH 6. The energy transfer distances are smaller than the hydrodynamic radius extracted from dynamic light scaterring. One possible explanation for this behavior is that the conjugation sites are presumably distributed throughout the dendrimer ligand coating, and hence the average distance for FRET will be shorter than that defined by the outer surfce of the coating. Despite the large size of the NC–SNARF dendrimer construct, the overall FRET efficiency is large owing to the high number of acceptor molecules at the NC surface. The high coupling yield suggests that primary amine sites are highly accessible from the aqueous solution, contrasting alternative amine–bearing ligand coatings in which competition of NC surface binding with solution display has been suspected.[36,37]

In order to determine the effectiveness of the NC–SNARF sensor in a biological–like environment, the construct was examined in 4% bovine serum albumin (BSA) in phosphate solutions buffered between pH 6.0 and pH 8.0 at 0.2 pH increments. Albumin was chosen as a blood mimic as it is generally the most abundant plasma protein in mammals;[38] in addition, BSA naturally introduces a mildly scattering optical environment, thus capturing a challenge in biological sensing. Fig 4a shows the pH dependence of the emission of the construct in BSA buffers. The BSA contributes a broad autofluorescence background but nonetheless the NC and SNARF emission peaks can be resolved clearly. The SNARF:NC integrated emission ratio decreases in the presence of BSA. NCs have previously been

shown to exhibit increased quantum yields when directly conjugated to BSA.[39,40] It has been suggested that BSA passivates the surface of the NCs by acting as a physical barrier of O_2 for surface oxidation.[40] Although our construct was only placed in a solution of BSA and not directly coupled, it is possible that the electrostatic attraction between the dendrimer coated NCs and BSA was strong enough to further passivate the NCs to increase their quantum yields. Note that in the absence of unconjugated NCs or direct excitation of the dye, changes in NC quantum yield alone will not change the FRET efficiency or the resulting emission ratio. On the other hand, the decrease in SNARF:NC emission ratio may be explained by a decrease in the quantum yield of the dye on its exposure to BSA. The pH calibration curve is significantly altered by the presence of BSA, however the range of sensitivity remains the same.

In a control experiment, matched concentrations of dendrimer coated NCs and SNARF–5F were individually placed in phosphate buffer with and without BSA buffer to see whether any differences existed in emission intensity. While dendrimer coated NCs exhibit approximately the same intensity, the intensity of SNARF–5F is diminished by approximately 90% (Fig S3). As albumin provides a hydrophobic environment, the diminished intensity of SNARF–5F may be due to solvent effects, a phenomenon commonly exhibited by xanthene–based dyes.[41–43] It is also possible that the dye may be forming a complex with the albumin, which has also been reported for fluorescein.[44] Given the high degree of quenching of SNARF–5F alone as compared to SNARF–5F covalently attached to the NC surface, conjugation of SNARF to the NC is beneficial as the NC scaffold mitigates SNARF interactions with the biological milieu.

We next examined whether sensing could be established under two–photon excitation (λ_{exc} = 800 nm). Fig 4b shows the two photon–excited fluorescence spectrum of the sensor under varying pH conditions, once again in phosphate buffers containing 4% BSA. The spectrum exhibits a ratiometric pH dependent profile, thus establishing that the FRET–based sensing scheme is viable for both one– and two–photon excitation. Notably, the BSA autofluorescence that was apparent under linear excitation was absent under 2-photon excitation at 800 nm. Despite the ratiometric response and absence of the BSA contribution, the emission lineshape differs quantitatively from that observed under linear excitation; the relative contribution of the dye emission is significantly larger under 2-photon excitation, particularly at high pH. Within a model for which excitation of the SNARF in the NC-SNARF construct occurs purely by energy transfer from the NC, the emission spectrum of the sensor should be independent of the excitation mode. The 2-photon action cross-sections of NCs are large compared to typical dyes and endogenous fluorophores. Indeed, action cross-sections of >10^4 Goppert-Meyer units for larger-diameter CdSe/ZnS NCs have been reported.[25] Our own measurements of a CdSe/CdZnS NC sample similar to the one used here, using a Rhodamine B standard, revealed a two-photon absorption cross-section of ~9000 Goppert-Meyer (GM) units at 800 nm excitation. With our value of F, an action cross-section of ~2300 GM units is expected for the NC donors in the sensor construct. At present, the origin of the deviation in sensor response between linear and 2-photon excitation is unclear, but it could be associated with direct two-photon excitation of the SNARF dye competing with FRET excitation under conditions where the NC is quenched or saturated.

The 2-photon excited fluorescence emission of the sensor in BSA-containing buffer was also detected using image-mode readout by using a dichroic filter centered at λ = 565 nm to direct the green (NC) and the red (SNARF) fluorescence emission channels onto two different PMT detectors. Fig S1b shows the calibration curve obtained with image mode detection under two–photon excitation; the results qualitatively replicate the monotonic increase of the SNARF:NC emission ratio with pH that was observed under linear excitation. pH changes as small as 0.2 pH units are detected at over 100 μm translation in depth.

Conclusions

We have demonstrated an effective CdSe/CdZnS NC based pH sensor that is effective in a physiologically relevant pH range. A poly(amido amine) scaffold has been incorporated as the capping ligand, which serves to impart water solubility and to furnish a high valency of primary amines for covalent coupling of multiple FRET acceptors. Both single– and two–photon excitation sources were found to be effective in eliciting pH–sensitive dual emission from the NC–SNARF conjugate. The accessibility of high ratios of acceptor molecules per NC to enhance the efficiency of energy transfer, the use of multiphoton excitation to minimize background signals and photodamage, and the ratiometric nature of the construct make the NC based sensor a promising tool for pH sensing in biological environments.

Supplementary Material

Refer to Web version on PubMed Central for supplementary material.

Acknowledgments

References

1. McLaurin EJ, Greytak AB, Bawendi MG, Nocera DG. J Am Chem Soc. 2009; 131:12994–13001. [PubMed: 19697933]

2. Medintz IL, Clapp AR, Mattoussi H, Goldman ER, Fisher B, Mauro JM. Nat Mater. 2003; 2:630–638. [PubMed: 12942071]

3. Somers RC, Bawendi MG, Nocera DG. Chem Soc Rev. 2007; 36:579–591. [PubMed: 17387407]

4. Snee PT, Somers RC, Nair G, Zimmer JP, Bawendi MG, Nocera DG. J Am Chem Soc. 2006; 128:13320–13321. [PubMed: 17031920]

5. Wang X, Boschetti C, Ruedas-Rama MJ, Tunnacliffe A, Hall EAH. Analyst. 2010; 135:1585–1591. [PubMed: 20449508]

6. Medintz IL, Stewart MH, Trammell SA, Susumu K, Delehanty JB, Mei BC, Melinger JS, Blanco-Canosa JB, Dawson PE, Mattoussi H. Nat Mater. 2010; 9:676–684. [PubMed: 20651808]

7. Murray CB, Norris DJ, Bawendi MG. J Am Chem Soc. 1993; 115:8706–8715.

8. Jaiswal JK, Simon SM. Tr Cell Biol. 2004; 14:497–504.

9. Hines MA, Guyot-Sionnest P. J Phys Chem. 1996; 100:468–471.

10. Clapp AR, Medintz IL, Mauro JM, Fisher BR, Bawendi MG, Mattoussi H. J Am Chem Soc. 2004; 126:301–310. [PubMed: 14709096]

11. Kagan CR, Murray CB, Nirmal M, Bawendi MG. Phys Rev Lett. 1996; 76:1517–1520. [PubMed: 10061743]

12. Clapp AR, Medintz IL, Fisher BR, Anderson GP, Mattoussi H. J Am Chem Soc. 2005; 127:1242–1250. [PubMed: 15669863]

13. Tomasulo M, Yildiz I, Raymo FM. J Phys Chem B. 2006; 110:3853–3855. [PubMed: 16509664]

14. Goldman ER, Medintz IL, Whitley JL, Hayhurst A, Clapp AR, Uyeda HT, Deschamps JR, Lassman ME, Mattoussi H. J Am Chem Soc. 2005; 127:6744–6751. [PubMed: 15869297]

15. Doussineau T, Schulz A, Lapresta-Fernandez A, Moro A, Koersten S, Trupp S, Mohr GJ. Chem Eur J. 2010; 16:10290–10299. [PubMed: 20665579]

16. Krooswyk JD, Tyrakowski CM, Snee PT. J Phys Chem C. 2010; 114:21348–21352.

17. Jain RK. Science. 2005; 307:58–62. [PubMed: 15637262]

18. Helmlinger G, Yuan F, Dellian M, Jain RK. Nat Med. 1997; 3:177–182. [PubMed: 9018236]

19. Jobsis PD, Rothstein EC, Balaban RS. J Microsc. 2007; 226:74–81. [PubMed: 17381712]

20. Clapp A, Pons T, Menditz IL, Delehanty JB, Melinger JS, Tiefenbrunn T, Dawson PE, Fisher BR, O'Rourke B, Mattoussi H. Adv Mater. 2007; 19:1921–1926.

21. Brown EB, Campbell RB, Tsuzuki Y, Xu L, Carmeliet P, Fukumura D, Jain RK. Nat Med. 2001; 7:864–868. [PubMed: 11433354]

22. Xu C, Zipfel W, Shear JB, Williams RM, Webb WW. Proc Natl Acad Sci USA. 1996; 93:10763–10768. [PubMed: 8855254]

23. König K. J Microsc. 2000; 200:83–104. [PubMed: 11106949]

24. Denk W, Strickler JH, Webb WW. Science. 1990; 248:73–76. [PubMed: 2321027]

25. Larson DR, Zipfel WR, Williams RM, Clark SW, Bruchez MP, Wise FW, Webb WW. Science. 2003; 300:1434–1436. [PubMed: 12775841]

26. Popovi Z, Liu W, Chauhan VP, Lee J, Wong C, Greytak AB, Insin N, Nocera DG, Fukumura D, Jain RK, Bawendi MG. Angew Chem Int Ed. 2010; 49:1–5.

27. Peng ZA, Peng X. J Am Chem Soc. 2001; 123:1389–1395.

28. Dabbousi BO, Rodriguez Viejo J, Mikulec FV, Heine JR, Mattoussi H, Ober R, Jensen KF, Bawendi MG. J Phys Chem B. 1997; 101:9463–9475.

29. Gunsalus IC, Barton LS, Gruber W. J Am Chem Soc. 1956; 78:1763–1766.

30. Wisher A, Bronstein I, Chechik V. Chem Commun. 2006:1637–1639.

31. Lakowicz JR, Gryczynski I, Gryczynski Z, Murphy CJ. J Phys Chem B. 1999; 103:7613–7620.

32. Aldana J, Wang YA, Peng XG. J Am Chem Soc. 2001; 123:8844–8850. [PubMed: 11535092]

33. Uyeda HT, Medintz IL, Jaiswal JK, Simon SM, Mattoussi H. J Am Chem Soc. 2005; 127:3870–3878. [PubMed: 15771523]

34. Liu W, et al. J Am Chem Soc. 2008; 130:1274–1284. [PubMed: 18177042]

35. Cakara D, Kleimann J, Borkovec M. Macromol. 2003; 36:4201–4207.

36. Han HS, Devaraj NK, Lee J, Jungmin, Hilderbrand SA, Weissleder R, Bawendi MG. J Am Chem Soc. 2010; 132:7838–7839. [PubMed: 20481508]

37. Liu W, Greytak AB, Lee J, Wong CR, Park J, Marshall LF, Jiang W, Curtin PN, Ting AY, Nocera DG, Fukumura D, Jain RK, Bawendi MG. J Am Chem Soc. 2010; 132:472–483. [PubMed: 20025223]

38. Quinlan GJ, Martin GS, Evans TW. Hepatology. 2005; 41:1211–1219. [PubMed: 15915465]

39. Gao XH, Chan WCW, Nie SM. J Biomed Opt. 2002; 7:532–537. [PubMed: 12421118]

40. Derfus AM, Chan WCW, Bhatia SN. Nano Lett. 2004; 4:11–18.

41. Fleming GR, Knight AWE, Morris JM, Morrison RJS, Robinson GW. J Am Chem Soc. 1977; 99:4306–4311.

42. Martin MM. Chem Phys Lett. 1975; 35:105–111.

43. Magde D, Rojas GE, Seybold PG. Photochem Photobiol. 1990; 70:737–744.

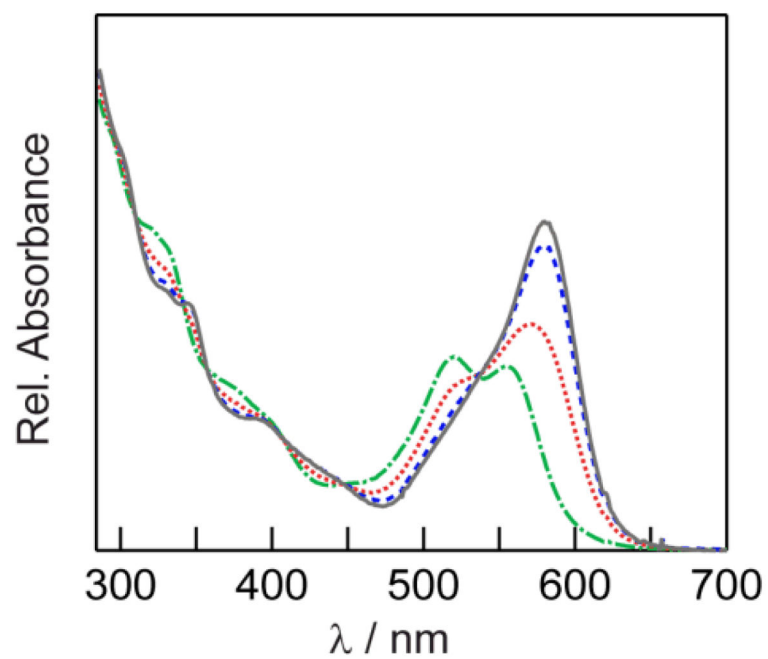44. Taarnhøj J, Schlecht L, McLaren JW, Brubaker RF. Exp Eye Res. 1990; 51:113–118. [PubMed: 2387331]

Fig. 1.
UV–vis absorbance spectra of NC–SNARF construct at pH 6 (green line — · ·), pH 7 (red line ···), pH 8 (blue line — —), and pH 9 (gray line —).
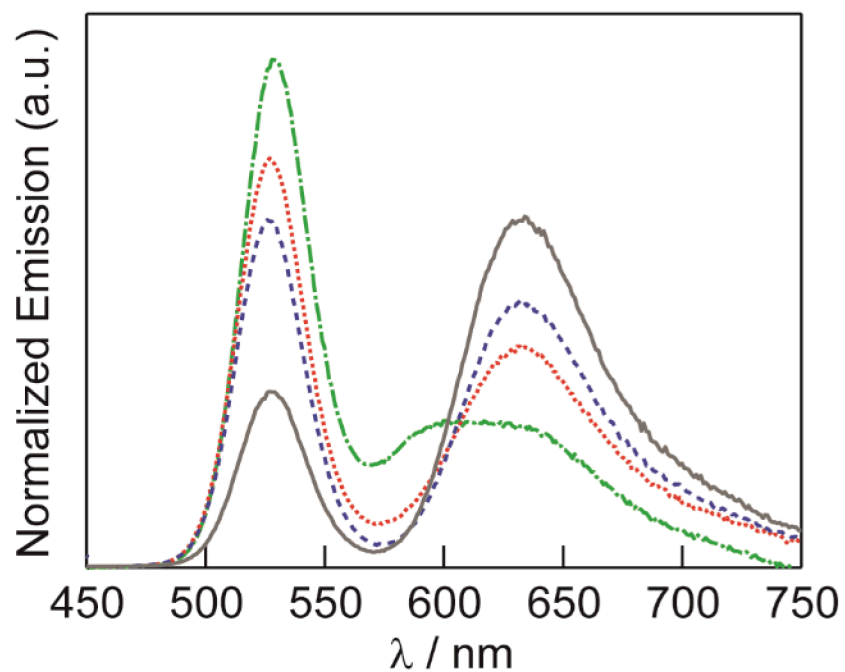
Fig. 2.
Normalized emission spectra of NC–SNARF construct in phosphate buffers at pH 6 (green line — ··), pH 7 (red line • • •), pH 8 (blue line — —), and pH 9 (gray line ——).NC emission decreases with a concomitant increase in dye emission with increasing pH.

Fig. 3.
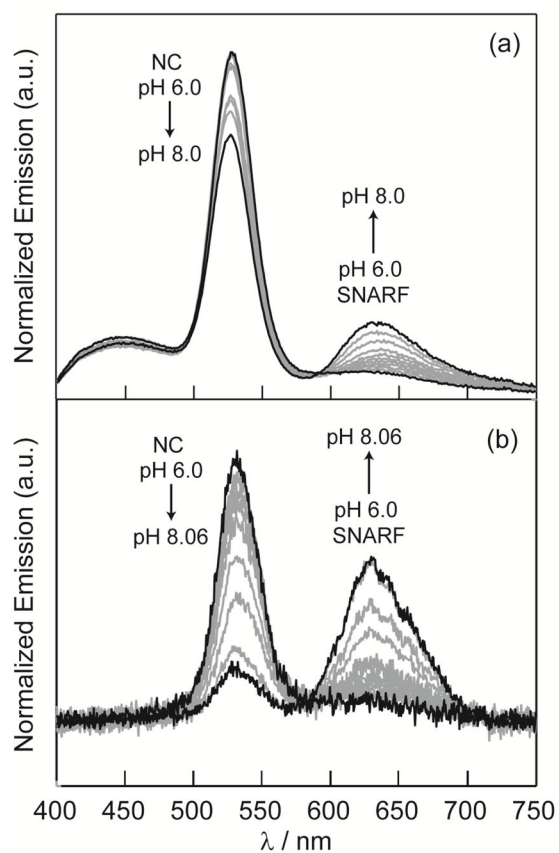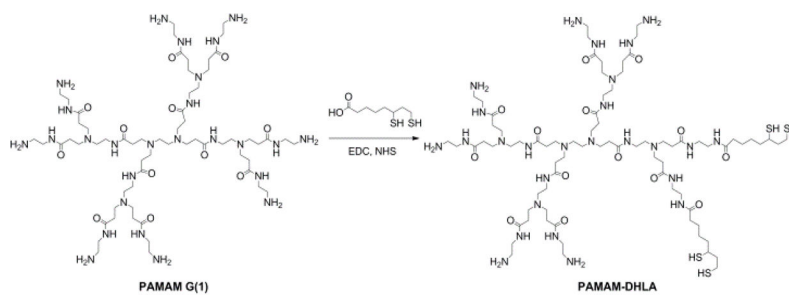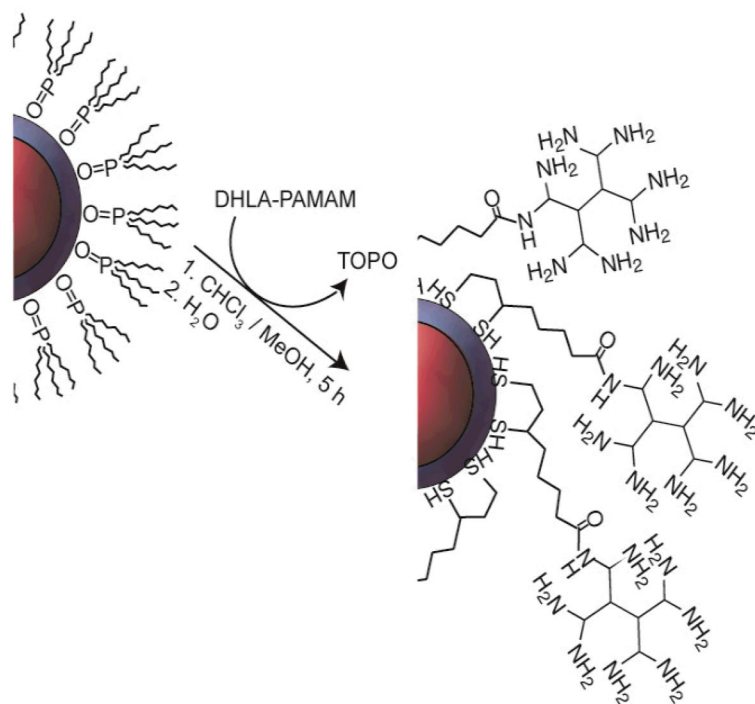Changes in emission color of the NC–SNARF sensor from left to right: pH = 6, 7, 8 and 9.

Fig. 4.
Normalized emission spectra of NC–SNARF in phosphate buffers containing 4% BSA under (a) one–photon excitation at 365 nm and (b) two–photon excitation at 800 nm. Spectra taken at 0.2 pH increments.

Scheme 1.

Scheme 2.

Table 1

Förster energy transfer parameters, dye to NC ratio, and size measurements for the NC–SNARF construct at different pH.

conjugate	τ / ns	R_0 / nm[a]	r / nm[b]	E / %[c]	m[d]
NC–SNARF pH 6	12	4.46	9.6	25	25
NC–SNARF pH 9	10	4.68	8.7	37.5	25

[a] Determined from fitting the Forster expression, see ESI.

[b] Determined from eq. 1.

[c] Determined from eq. 2.

[d] Determined from deconstructing the UV–vis spectra.